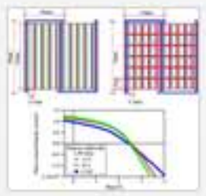

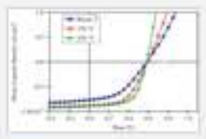

Table 1

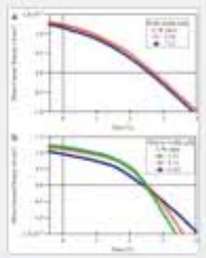

Table 2

Solar Energy Materials and Solar Cells
Volume 116, September 2013, Pages 219–223

Module structure for an organic photovoltaic device

Nam Su Kang[a], Byeong-Kwon Ju[a], Jae-Woong Yu[b]

Highlights

- Influences of module design on the performance of OPV modules were studied.
- As the longitudinal partitioning of cell increases, the performance of the module increases.
- The optimum cell length to width ratio was between 16 and 18.

Abstract

The influence of module design on the performance of OPV modules was studied, especially longitudinal partition effects. Two different module designs were used, one with wider cells (8 mm) and one with narrower cells(3.7 mm).The narrow structure had a current extraction metal sub-electrode in the middle of the module, and a tandem series connection of 4 or 5 cells was used for a fixed total module area. The current density, fill factor, shunt resistance, and power conversion efficiency of the narrow cells were higher than those of the wide cells with a comparable length-to-width ratio. As the longitudinal partitioning of a cell increases, the performance of the device increases. However, the effective active area of the module decreases, so the total power output will decrease. The optimum length-to-width ratio of wide or narrow cells is between 16 and 18.

Graphical abstract

Solar Energy Materials & Solar Cells 116 (2013) 219–223

Contents lists available at SciVerse ScienceDirect

Solar Energy Materials & Solar Cells

journal homepage: www.elsevier.com/locate/solmat

Module structure for an organic photovoltaic device

Nam Su Kang [a], Byeong-Kwon Ju [a], Jae-Woong Yu [b,*]

[a] Display and Nanosystem Laboratory, College of Engineering, Korea University, Seoul 136-713, Republic of Korea
[b] Department of Advanced Materials Engineering for Information & Electronics, Kyung Hee University, 1732 Deogyeong-daro, Giheung-gu, Yongin, Gyeonggi 446-701, Republic of Korea

ARTICLE INFO

Article history:
Received 20 December 2012
Received in revised form
24 April 2013
Accepted 7 May 2013
Available online 6 June 2013

Keywords:
Organic photovoltaic
Polymer solar cell
Module
Shunt resistance
Fill Factor

ABSTRACT

The influence of module design on the performance of OPV modules was studied, especially longitudinal partition effects. Two different module designs were used, one with wider cells (8 mm) and one with narrower cells(3.7 mm).The narrow structure had a current extraction metal sub-electrode in the middle of the module, and a tandem series connection of 4 or 5 cells was used for a fixed total module area. The current density, fill factor, shunt resistance, and power conversion efficiency of the narrow cells were higher than those of the wide cells with a comparable length-to-width ratio. As the longitudinal partitioning of a cell increases, the performance of the device increases. However, the effective active area of the module decreases, so the total power output will decrease. The optimum length-to-width ratio of wide or narrow cells is between 16 and 18.

1. Introduction

Organic photovoltaics (OPVs) are attractive alternatives to conventional inorganic semiconductor-based photovoltaics, because they are light weight, mechanically flexible, compatible with flexible substrates, and large area device can be fabricated at low cost. Due to the strong demand for cheap, renewable energy, OPVs have been the subject of increasing developments over the last decade [1–8]. Recent rapid improvements in the power conversion efficiency (up to 10.6%) [4] have increased the anticipation for commercial OPV devices in the near future.

To deliver the electrical power needed for applications, a module structure with connections between each subcell is needed to increase the output power. Creating a series of connected modules is an easy way to increase power output. The first series connection in an OPV was a tandem cell consisting of phthalocyanine and perylenetetracarboxylic derivate, which approximately doubled the open circuit voltage compared to a single solar cell [9]. This study reports a series connection within a unit cell. Lungenschmied et al. [10] reported the first meaningful geometrical OPV modules, with square, broad-stripe, and narrow-stripe geometries. However, the dimensions were not practical for fabricating actual modules. Lyu et al. [11] reported an efficiency change according to the module structure using a theoretical power loss model. They used a series tandem structure module with 4 different widths (18.6, 11.6, 8.1, and 6.0 mm), and concluded that the optimum active cell was 13 mm wide. Many studies have assessed the effects of cell geometry on unit cell performance, but there have been relatively few studies on the effects of module geometry [10–17]. In a shading test of OPV modules, 10% shading shut down the whole module [17]. Therefore, optimum designs are critical to produce the maximum power output from a given module area. Krebs et al. reported several studies on the effects of module structure on the performance of roll-to-roll processed polymer solar cells [8,18–20]. The module structure of a polymer solar cell with a serially connected ITO stripe having different widths was studied. It was concluded that the width should be narrowest for a low series resistance, and widest for the active area [18]. They showed that the increased performance of OPV by narrowing the stripe width was quickly lost due to a loss in active area.

All of the module studies so far have concentrated only on the influence of the lateral direction, since charges have to traverse series connections to produce electricity. We investigated the influence of module design on the performance of OPV modules. In particular, we studied the influence of longitudinal partitions on module performance. We demonstrate that longitudinal partitioning is universally applicable to all organic photovoltaic modules.

2. Materials and methods

2.1. Fabrication of devices

A patterned ITO panel for cell testing was prepared by photolithography and cleaned by acetone, isopropyl alcohol, and

* Corresponding author. Tel.: +82 31 201 3325; fax: +82 31 204 8114.
E-mail address: jwyu@khu.ac.kr (J.-W. Yu).

0927-0248/$ - see front matter © 2013 Elsevier B.V. All rights reserved.
http://dx.doi.org/10.1016/j.solmat.2013.05.009

deionized water. Molybdenum oxide was deposited by thermal vapor deposition at 7×10^{-7} Torr and annealed at 250 °C in a nitrogen dry box for use as a hole transfer layer.

A typical organic solar cell module was prepared as follows: a blend containing 2.4 wt% P3HT (purchased from Rieke Metals, EE grade) and PCBM (purchased from Nano-C) with a 1:0.6 weight ratio was dissolved in anhydrous chlorobenzene and spin-coated at 2500 rpm for 40 s onto ITO glass coated with a molybdenum oxide layer. The resulting active layer was 140 nm thick, and was pre-annealed at 120 °C for 10 min. A 0.8 nm thick LiF layer was deposited as a buffer for electron extraction on top of the active layer, and a 150 nm thick aluminum layer was deposited by thermal vapor deposition at 10^{-6}–10^{-7} Torr. The prepared device was post-annealed at 120 °C for 10 min.

2.2. Fabrication of modules

A 10 cm × 10 cm piece of ITO glass with a sheet resistance of 8 Ω/□ was prepared from a large piece of ITO glass, and photolithography was used to create the desired pattern. The prepared ITO glass was then cleaned by rinsing with several solvents (acetone, isopropyl alcohol, and deionized water) and dried in a vacuum oven at a temperature of 200 °C. The ITO glass was treated with ozone for 15 min just before use. The hole transporting layer (MoO_x) was deposited at high vacuum (5×10^{-7} Torr) by thermal deposition (with a deposition rate of 1 Å/s). The 30 nm thick MoO_x layer was annealed for 30 min on a 250 °C hot plate inside a glove box with an N_2 atmosphere. The active layer stock solution (concentration: 2.5 wt%, with a donor acceptor ratio of 1:0.6) was spin coated at 900 rpm for 5 s inside a glove box, and also annealed on a hot plate at 120 °C for 30 min. A 150 nm thick aluminum layer was applied by thermal vapor deposition at 10^{-6}–10^{-7} Torr, and the prepared device was post-annealed at 120 °C for 10 min.

2.3. Characterizations

The thickness of the coated film was measured with a surface profiler (TENCOR®, P-10 α-step). The absorption spectra of the films were obtained using a photodiode array type UV–vis spectrometer (HP 8453). An Oriel Class A solar simulator (IEC 904) with an Oriel Reference Cell (calibrated data traceable to NREL) was used as a light source. All measurements were performed under a 1 sun condition (AM1.5 100 mW/cm^2). Measurements were not corrected for reflection loss or light absorption in the ITO electrode. The *I–V* characteristics were determined with a Keithley 2400 source-measure unit.

3. Results and discussion

A MoO_x layer was used as a hole transporting layer instead of the typical conducting polymer film (PEDOT), since thermally evaporated MoO_x provides better smoothness and stability. Thermally evaporated MoO_x provides a more uniform thickness than spin-coated polymer films in 10 cm × 10 cm modules. Additionally, the acidity of PEDOT solution reduces the lifetime of organic photovoltaic devices [8,21,22]. The conductivity of MoO_x is lower than that of PEDOT film, but it can be improved by enhancing the oxygen vacancies, which is easy at relatively low temperature (250 °C) [23]. Fig. 1 shows the *I–V* characteristics of 2 mm × 2 mm devices with thermally treated MoO_x layers. The device performance was enhanced as the annealing temperature was increased. The reasons for these enhancements include the enhancement of the layer roughness by baking, and the creation of oxygen vacancies improving the electron and hole mobilities. As a result,

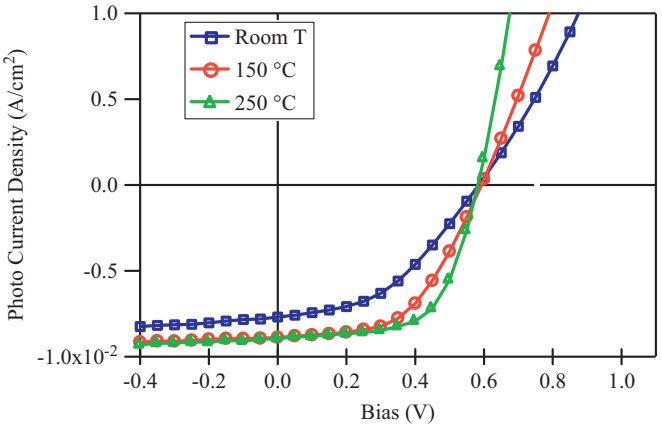

Fig. 1. *I–V* characteristics of thermally treated MoO_x layers.

Table 1
Performance of devices with annealed MoOx.

Annealing *T* (°C)	J_{sc} (mA/cm^2)	V_{oc} (V)	FF	PCE (%)
Room T	7.69	0.58	0.44	1.96
150	8.87	0.59	0.52	2.76
250	9.06	0.58	0.65	3.41
PEDOT reference	8.86	0.59	0.65	3.40

the device prepared on a MoO_x layer annealed for 30 min at 250 °C had identical performance to a device prepared on PEDOT film, as summarized in Table 1. The annealed device showed markedly enhanced power performance compared to the as-prepared device (representing an enhancement in efficiency of about 70%, from 1.96 to 3.41).

Fig. 2 shows the module designs used in this study. We used two different designs: one with wider cells (8 mm) and one with narrower cells (3.7 mm). The module size was fixed at 10 cm × 10 cm. Using identical processing techniques (i.e., the same distance between cells), the wide-cell module has a higher effective cell area (22.8 and 21.6 cm^2) than the narrow-cell module (18.6, 17.8, and 16.9 cm^2). The wide-cell module has 5 cells connected in series to produce an open circuit voltage of about 2.6–2.7 V, while the narrow-cell module had 4 cells connected in series to produce about 2.4–2.5 V. The narrow structure has a current extraction metal sub-electrode in the middle of module to produce more current with a similar open circuit voltage compared to the wide structure (i.e. 4 cells connected in series with a current extraction metal sub-electrode in the middle).

Fig. 3(a) and (b) shows the *I–V* characteristics of the modules with wide and narrow cells, respectively. As the longitudinal partitioning of the cell increased (i.e., the length-to-width ratio decreased), the current density, fill factor, and shunt resistance increased. The results are summarized in Table 2. In the wide-cell module, as the length-to-width ratio decreased from 7.125 (57 mm long × 8 mm wide) to 3.375 (27 mm long × 8 mm wide), the series resistance did not change, and the fill factor increased slightly. However, the short circuit current density increased by about 6% and the shunt resistance increased by about 40%. As a result of these changes, the power conversion efficiency increased by about 13% (from 0.99 to 1.12). In the narrow-cell module, as the length-to-width ratio decreased from 17.027 (63 mm long × 3.7 mm wide) to 2.568 (9.5 mm long × 3.7 mm wide), all characteristics increased. The current density increased by 25%, the fill factor increased by 13%, the shunt resistance increased by 110%, the series resistance increased by 45%, and the power conversion efficiency increased by 45%. Comparing the analogous length-to-width ratios between

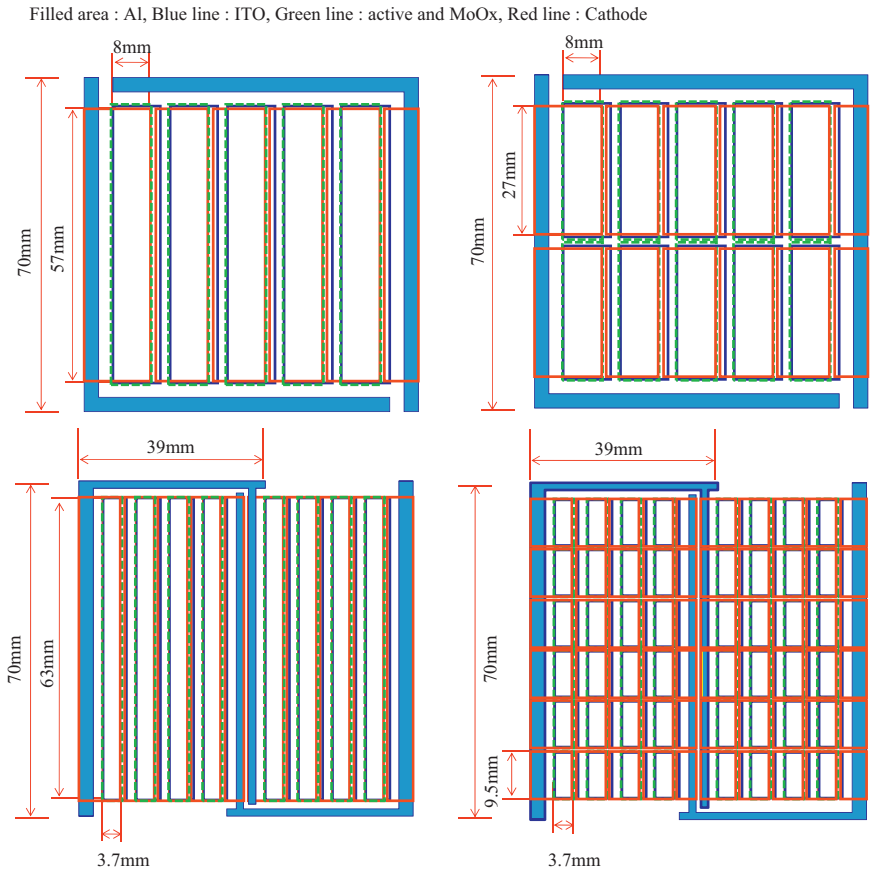

Fig. 2. Module designs used in this study.

the narrow- and wide-cell modules, the fill factor, shunt resistance, and power conversion efficiency of the narrow-cell modules were higher than that of the wide-cell module.

Fig. 4 shows a plot of the short circuit current density (the experimental errors included) vs. the length-to-width ratio. The short circuit current density was slightly higher for the wide-cell module. In the wide cell, the short circuit current density was increased by about 6% (from 1.16 to 1.23) by reducing the length-to-width ratio from 7.125 to 3.375. In the narrow cell, the short circuit current density increased by about 5% (from 1.12 to 1.18) with a comparable reduction in the length-to-width ratio (from 8.108 to 2.568). The cell structure in this study is a tandem series connection of 4 or 5 cells, and thus, the transverse distance for a charge is lower for narrow cells, and the short circuit current density should be higher. Lungenschmied et al. [10] reported a rapid decrease in device efficiency with increasing cell width. In this study, however, due to the power extraction sub-electrode for the narrow-cell module and the poor charge extraction efficiency due to the contact resistance, the short circuit current density decreased slightly for the narrow-cell module. Comparing modules with the same structure, the short circuit current density decreased as the length-to-width ratio increased within the same-width module. In other words, charge production is more efficient when there is more partitioning within the cells due to the reduced series resistance and increased shunt resistance. Lyu et al. [11] reported that the optimum active cell length was 13 mm; however, in our study, the narrow cell (3.7 mm) had better performance than the wide cell (8 mm), and both are narrower than the suggested optimum.

Fig. 5 shows the module characteristics (the experimental errors included) vs. the length-to-width ratio. As shown in Fig. 5(a), the shunt resistance of the narrow-cell module is higher than that of the wide-cell module, resulting in higher power conversion efficiency, as shown in Fig. 5(c). The fill factors for the narrow-cell modules are about 30% higher than those of the wide-cell modules. This phenomenon is reasonable, since the diode factor for the narrow-cell modules should be better due to the shorter distance for extracted charges to travel and the deleterious effect of the lateral contributions of the series resistance from other active areas to the bulk resistance. The shunt resistance of the narrow-cell module decreases as the length-to-width ratio increases, which implies that modules with long stripes have lower shunt resistance, and therefore, lower power conversion efficiency. As shown in Fig. 5(c), the power conversion efficiency increased as the length-to-width ratio decreased (i.e., as partitioning increased). The relative ratio of this efficiency increment is higher when the cell is narrow. Therefore, the power conversion efficiency is higher for modules with more partitioning.

Among the device parameters related to power output, the series resistance is more influenced by the materials used for fabrication. The fill factor and the shunt resistance are related to the diode factor, which dictates power loss. As shown in Fig. 5 (a) and (b), the shunt resistance and fill factor increased with increased partitioning in both modules (narrower and wider). From the shunt resistance plot (Fig. 5(a)), when we extrapolate to zero shunt resistance, the length-to-width ratio is about 17 for both narrow and wide cells. Accounting for experimental error, the optimum length-to-width ratio should be between 16 and 18. Since the shunt resistance is a key factor for efficient power conversion, the length-to-width ratio should be optimal to obtain maximum power from a given module geometry. Again, as cell partitioning increases, the device performance increases, however, the available effective active area within the module and total output decrease.

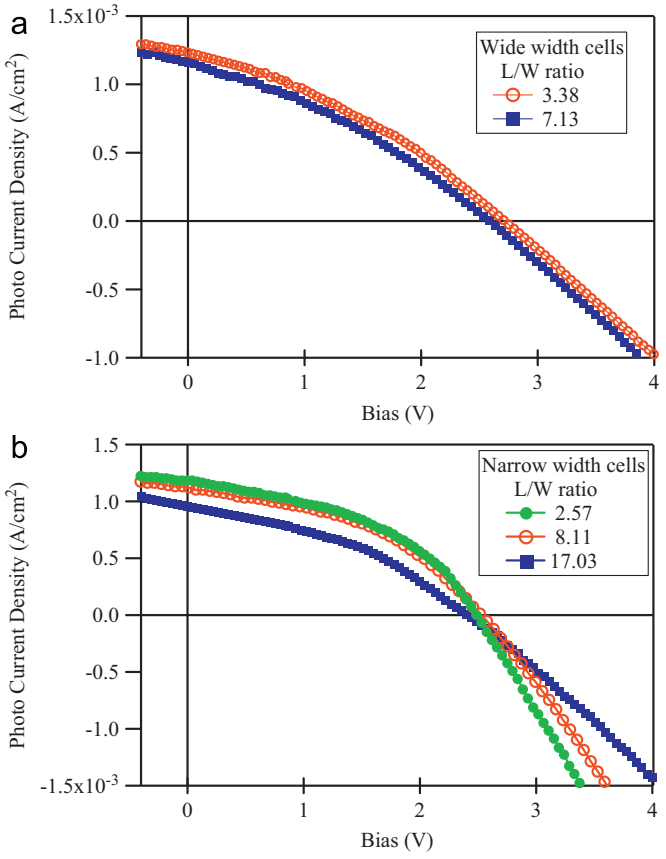

Fig. 3. (a) *I–V* characteristics of the module fabricated with wide width cells. (b) *I–V* characteristics of the module fabricated with narrow width cells.

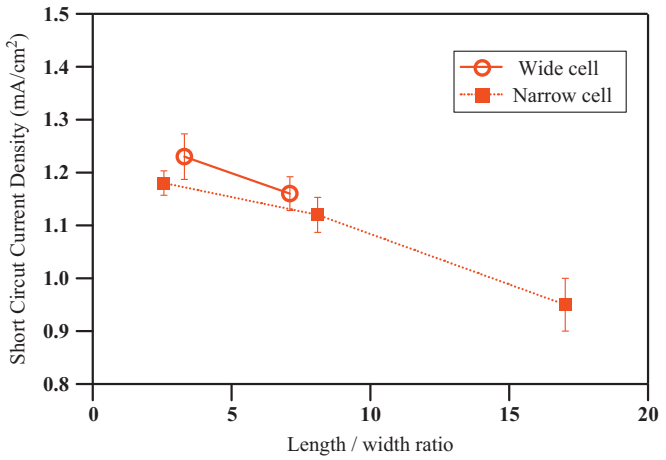

Fig. 4. Plot of length-to-width ratio vs. the current density.

4. Conclusions

The influence of longitudinal partitioning on OPV module performance was studied. Wide-cell modules (8 mm cells) and

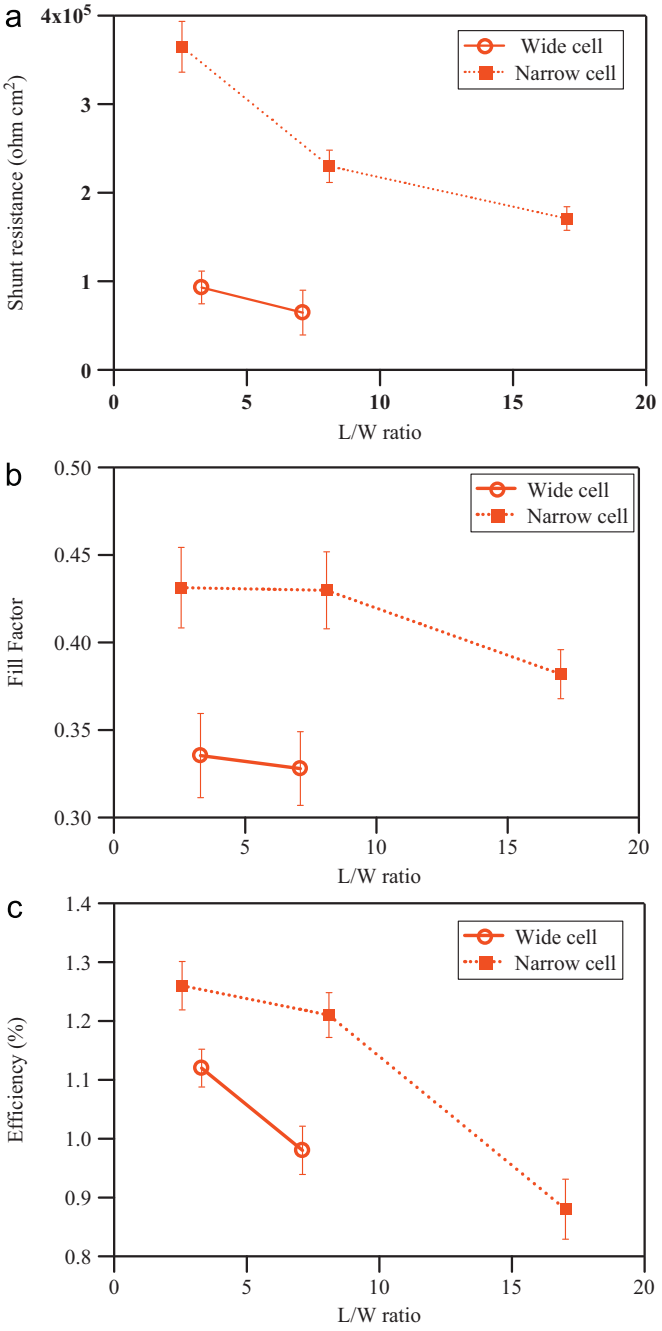

Fig. 5. (a) Plot of length-to-width ratio vs. shunt resistance; (b) plot of length-to-width ratio vs. fill factor; and (c) plot of length-to-width ratio vs. efficiency.

Table 2
Results of longitudinal partitioning.

	L/W ratio	Device area (cm^2)	J_{sc} (mA/cm^2)	FF	R_{sh} (Ωcm^2)	R_s (Ωcm^2)	PCE (%)
Wide	7.125	22.8	1.16 ± 0.03	0.328 ± 0.020	64550 ± 25310	1300 ± 130	0.99 ± 0.04
	3.375	21.6	1.23 ± 0.04	0.335 ± 0.025	92900 ± 18430	1325 ± 150	1.12 ± 0.03
Narrow	17.027	18.6	0.95 ± 0.05	0.382 ± 0.014	170800 ± 13240	1100 ± 90	0.88 ± 0.05
	8.108	17.8	1.12 ± 0.03	0.430 ± 0.023	229800 ± 18230	650 ± 37	1.22 ± 0.04
	2.568	16.9	1.18 ± 0.02	0.431 ± 0.027	364700 ± 28620	590 ± 41	1.27 ± 0.04

narrow-cell modules (3.7 mm cells) were used to form modules with a fixed area. The narrow-cell module performed better than the wide-cell module. As the longitudinal partitioning increased, the device performance increased. Increased cell partitioning, however, decreased the effect of the active area due to the space required for partitioning. As a result, the total power output decreased. The optimum length-to-width ratio in both wide and narrow cells was between 16 and 18, within the experimental error. This method can be universally applied to organic photovoltaic modules to maximize output.

Acknowledgments

This research was supported by the Basic Science Research Program through the National Research Foundation of Korea (NRF) funded by the Ministry of Education, Science and Technology (2010–0007122).

References

[1] W.L. Ma, C.Y. Yang, X. Gong, K. Lee, A.J. Heeger, Thermally stable, efficient polymer solar cells with nanoscale control of the interpenetrating network morphology, Advanced Functional Materials 15 (2005) 1617–1622.
[2] J.Y. Kim, K. Lee, N.E. Coates, D. Moses, T.Q. Nguyen, M. Dante, A.J. Heeger, Efficient tandem polymer solar cells fabricated by all-solution processing, Science 317 (2007) 222–225.
[3] Y. Liang, Z. Xu, J. Xia, S.-T. Tsai, Y. Wu, G. Li, C. Ray, L. Yu, For the bright future—bulk heterojunction polymer solar cells with power conversion efficiency of 7.4%, Advanced Materials 22 (2010) 1–4.
[4] G. Li, R. Zhu, Y. Yang, Polymer solar cells, Nature Photon 22 (2010) 1–4.
[5] C.W. Schlenker, M.E. Thompson, Current challenge in organic photovoltaic solar energy convrsion, Topics in Current Chemistry 312 (2012) 175–212.
[6] R. Gaudiana, Organic photovoltaics: challenge and opportunities, Journal of Polymer Science Part B: Polymer Physics 50 (2012) 1014–1017.
[7] M. Jørgenson, K. Norrman, S.A. Gevorgyan, T. Tromholt, B. Andreasen, F. C. Krebs, Stability of polymer solar cells, Advanced Materials 24 (2012) 580–612.
[8] R.R. Søndergaard, M. Hösel, F.C. Krebs, Roll-to-roll fabrication area functional organic materials, Journal of Polymer Science Part B: Polymer Physics 51 (2013) 16–34.
[9] M. Hiramoto, M. Suezaki, M. Yokoyama, Effect of thin gold interstitial-layer on the photovoltaic properties of tandem organic solar cell, Chemistry Letters 19 (1990) 327–330.
[10] C. Lungenschmied, G. Dennler, H. Neugebauer, S.N. Sariciftci, M. Glatthaar, T. Meyer, A. Meyer, Flexible, long-lived, large-area, organic solar cells, Solar Energy Materials and Solar Cells 91 (2007) 379–384.
[11] H.K. Lyu, J.H. Sim, S.-H. Woo, K.P. Kim, J.-K. Shin, Y.S. Han, Efficiency enhancement in large-area organic photovoltaic module using theoretical power loss model, Solar Energy Materials and Solar Cells 95 (2011) 2380–2383.
[12] B. Zimmermann, M. Glatthaar, M. Niggemann, M.K. Riede, A. Hinsch, A. Gombert, ITO-free wrap through organic soalr cells—a module concept for cost-efficient reel-to-reel production, Solar Energy Materials and Solar Cells 91 (2007) 374–378.
[13] F.C. Krebs, H. Spanggard, T. Kjaer, M. Biancardo, J. Alstrup, Large area plastic solar cell modules, Materials Science and Engineering B138 (2007) 106–111.
[14] M. Niggemann, B. Zimmermann, J. Haschke, M. Glatthaar, A. Gombert, Organic solar cell modules for specific applications—from energy autonomous systems to large area photovoltaics, Thin Solid Films 516 (2008) 7181–7187.
[15] B. Muhsin, J. Renz, K.-H. Drüe, G. Gobsch, H. Hoppe, Influence of polymer solar cell geometry on series resistance and device efficiency, Physica Status Solidi A 206 (2009) 2771–2774.
[16] R. Tipnis, J. Bernkopf, S. Jia, J. Krieg, S. Li, M. Storch, D. Laird, Solar Energy Materials and Solar Cells 93 (2009) 442–446.
[17] R. Steim, P. Schilinsky, S.A. Choulis, C.J. Brabec, Flexible polymer photovoltaic modules with incorporated organic bypass diodes to address module shading effects, Solar Energy Materials and Solar Cells 93 (2009) 1963–1967.
[18] F.C. Krebs, T. Tromholt, M. Jørgensen, Upscaling of polymer solar cell fabrication using full roll-to-roll processing, Nanoscale 2 (2010) 873–886.
[19] ITO-free flexible polymer soalr cells: from small model devices to roll-to-roll processed large modules, Organic Electronics, 12 (2011) 566–574.
[20] N. Espinosa, R. García-Valverde, A. Urbina, F. Lenzmann, M. Manceau, D. Angmo, F.C. Krebs, Life cycle assessment of ITO-free flexible polymer solar cells prepared by roll-to-roll coating and printing, Solar Energy Materials and Solar Cells 97 (2012) 3–13.
[21] J.-C. Wang, W.-T. Weng, M.-Y. Tsai, M.-K. Lee, S.-F. Horng, T.-P. Perng, C.-C. Kei, C.-C. Yu, H.-F. Meng, Highly efficient flexible inverted organic solar cells using atomic layer deposited ZnO as electron selective layer, Journal of Materials Chemistry 20 (2010) 862–866.
[22] K. Kawano, R. Pacios, D. Poplavskyy, J. Nelson, D. Bradley, J.R. Durrant, Degradation of organic solar cells due to air exposure, Solar Energy Materials and Solar Cells 90 (2006) 3520–3530.
[23] S.-Y. Lin, Y.-CPlease check the edit(s) made in author group (Y.C.g Chen is changed to Y.C.Chen), and kindly correct if necessary.. Chen, C.-M. Wang, P.-T. Hsieh, S.-C. Shih, Post-annealing effect upon optical properties of electron beam evaporated, Applied Surface Science 255 (2009) 3868–3874.